A complex of Arabidopsis DRB proteins can impair dsRNA processing

A complex of *Arabidopsis* DRB proteins can impair dsRNA processing

MARIE-AUDE TSCHOPP,[1] TAICHIRO IKI,[1,2] CHRISTOPHER A. BROSNAN,[1] PAULINE E. JULLIEN,[1,3] and NATHAN PUMPLIN[1,4]

[1]Department of Biology, ETH Zürich, 8092 Zürich, Switzerland
[2]Graduate School of Frontier Biosciences, Osaka University, Osaka 565-0871, Japan
[3]IRD, 34394 Montpellier, France

ABSTRACT

Small RNAs play an important role in regulating gene expression through transcriptional and post-transcriptional gene silencing. Biogenesis of small RNAs from longer double-stranded (ds) RNA requires the activity of dicer-like ribonucleases (DCLs), which in plants are aided by dsRNA binding proteins (DRBs). To gain insight into this pathway in the model plant *Arabidopsis*, we searched for interactors of DRB4 by immunoprecipitation followed by mass spectrometry-based fingerprinting and discovered DRB7.1. This interaction, verified by reciprocal coimmunoprecipitation and bimolecular fluorescence complementation, colocalizes with markers of cytoplasmic siRNA bodies and nuclear dicing bodies. In vitro experiments using tobacco BY-2 cell lysate (BYL) revealed that the complex of DRB7.1/DRB4 impairs cleavage of diverse dsRNA substrates into 24-nucleotide (nt) small interfering (si) RNAs, an action performed by DCL3. DRB7.1 also negates the action of DRB4 in enhancing accumulation of 21-nt siRNAs produced by DCL4. Overexpression of DRB7.1 in *Arabidopsis* altered accumulation of siRNAs in a manner reminiscent of *drb4* mutant plants, suggesting that DRB7.1 can antagonize the function of DRB4 in siRNA accumulation in vivo as well as in vitro. Specifically, enhanced accumulation of siRNAs from an endogenous inverted repeat correlated with enhanced DNA methylation, suggesting a biological impact for DRB7.1 in regulating epigenetic marks. We further demonstrate that RNase three-like (RTL) proteins RTL1 and RTL2 cleave dsRNA when expressed in BYL, and that this activity is impaired by DRB7.1/DRB4. Investigating the DRB7.1–DRB4 interaction thus revealed that a complex of DRB proteins can antagonize, rather than promote, RNase III activity and production of siRNAs in plants.

Keywords: double-stranded RNA binding protein (DRB); RNase III; RNase three-like; in vitro BY-2 lysate; RNA silencing; DCL; endogenous inverted repeats

INTRODUCTION

RNA silencing mechanisms broadly regulate gene expression in eukaryotes. In plants, post-transcriptional gene silencing (PTGS) and transcriptional gene silencing (TGS) regulate key steps in development, stress adaptation, and pathogen defense through small RNAs, which are loaded into Argonaute proteins to effect sequence-guided silencing against mRNAs or chromatin, respectively. (Martínez de Alba et al. 2013; Bologna and Voinnet 2014; Borges and Martienssen 2015). Small RNAs are processed from longer double-stranded (ds) RNA by a specialized, conserved class of dual RNase III domain-containing ribonucleases of the Dicer family, aided in plants by interactions with double-stranded RNA binding proteins (DRBs) (Bernstein et al. 2001; Curtin et al. 2008). Animal Dicer proteins also recruit dsRNA binding proteins to process small RNAs, including *Caenorhabditis elegans* RDE-4, *Drosophila spp.* Loquacious, and mammalian TRBP and PACT (Ha and Kim 2014).

The model plant *Arabidopsis thaliana* encodes four DICER-LIKE proteins (DCLs) and five DRB members containing dual dsRNA binding motifs (dsRBM) (Schauer et al. 2002; Clavel et al. 2016). DCL1 produces micro (mi) RNAs from short hairpin precursors that form imperfect stem–loop structures (Park et al. 2002; Reinhart et al. 2002; Kurihara and Watanabe 2004). DCL1 requires an interaction with DRB1/HYL1 for efficient and precise mature miRNA production and loading (Kurihara et al. 2006; Dong et al. 2008; Eamens et al. 2009). DRB2 can also bind DCL1, and acts in miRNA biogenesis to favor silencing action *via* translational repression over transcript cleavage (Hiraguri

[4]**Present address: Department of Plant Sciences, University of California, Davis, CA 95616, USA**
Corresponding author: npumplin@ethz.ch
Article is online at http://www.rnajournal.org/cgi/doi/10.1261/rna.059519.116.

et al. 2005; Reis et al. 2015), and DRB2 also associates with chromatin regulators and binds transposable element (TE) transcripts (Clavel et al. 2015).

The remaining DCLs generate small-interfering (si) RNAs from perfectly- or near-perfectly complementary dsRNA precursors, which arise from the activity of RNA-dependent RNA polymerases (RDRs), transcription of stem–loop inverted repeats (IRs) or the presence of exogenous dsRNA such as that formed during viral infections (Dunoyer et al. 2005; Gasciolli et al. 2005; Xie et al. 2005; Henderson et al. 2006). DCL4 generates 21-nucleotide (nt) *trans*-acting (ta) siRNAs from endogenous *TAS* transcripts following dsRNA synthesis by RDR6 (Vazquez et al. 2004; Gasciolli et al. 2005; Xie et al. 2005; Yoshikawa et al. 2005; Adenot et al. 2006; Arribas-Hernández et al. 2016). DCL4 also processes young miRNAs with perfect or near-perfect self-complementary stem–loop precursors (Allen et al. 2004; Rajagopalan et al. 2006; Fahlgren et al. 2007), and is the primary antiviral DCL in *Arabidopsis* (Blevins et al. 2006; Bouche et al. 2006; Deleris et al. 2006; Diaz-Pendon et al. 2007). This locus can be expressed as two different isoforms: A longer mRNA encodes a nuclear localization signal ($DCL4^{NLS}$), and a shorter transcript bypasses the NLS sequence ($DCL4^{\Delta}$) (Pumplin et al. 2016). DCL4 activity is facilitated by its interacting partner DRB4, which is required for the proper biogenesis of tasiRNAs and young miRNAs, as well as antiviral silencing and localization in nuclear dicing bodies (Hiraguri et al. 2005; Adenot et al. 2006; Rajagopalan et al. 2006; Nakazawa et al. 2007; Curtin et al. 2008; Qu et al. 2008; Eamens et al. 2009; Fukudome et al. 2011; Jakubiec et al. 2012; Pumplin et al. 2016). DCL2, which does not have a known interaction with a DRB protein, is involved in producing secondary, 22-nt-long siRNAs with DCL4 during transitivity, and it also functions in a hierarchal manner as a backup to DCL4 and DCL3 on dsRNA generated by viruses, transgene hairpins, and endogenous dsRNA (Gasciolli et al. 2005; Deleris et al. 2006; Fusaro et al. 2006; Moissiard et al. 2007; Parent et al. 2015). DCL2 also generates 22-nt siRNAs from endogenous inverted repeats, which are hairpin sequences encoded in the *Arabidopsis* genome by loci such as *IR71* and *IR2039* (Henderson et al. 2006). The biological function of IRs remains obscure, but their processing patterns are impacted by mutation of *DRB* genes, such that the major population of siRNAs shifts from 22-nt-long siRNAs in WT to 24-nt in *drb4* or *drb7.2* mutants (Pelissier et al. 2011; Montavon et al. 2016). Finally, DCL3 functions in TGS via RNA-directed DNA methylation (RdDM) (Xie et al. 2004; Law and Jacobsen 2010; Matzke et al. 2014), by producing 24-nt siRNAs from endogenous or exogenous hairpin dsRNA and also p4-siRNAs, so called because their endogenous ~30- to 40-nt dsRNA precursors are synthesized by RNA Polymerase IV, together with RDR2 (Mosher et al. 2009; Blevins et al. 2015; Zhai et al. 2015). RdDM can initiate DNA methylation in all sequence contexts (CG, CHG, and CHH, where H is any nucleotide except G), and it is also the major pathway responsible to maintain CHH methylation (Law and Jacobsen 2010; Matzke et al. 2014). DRB3 interacts with DCL3 and participates in defense against DNA viruses (Raja et al. 2014).

In addition to DCLs, dsRNA can also be cleaved by a family of RNase three-like proteins (RTLs), which contain one or more RNase III domain. In *Arabidopsis*, RTL1 and RTL2 process long dsRNAs and influence small RNA accumulation and function. Plants overexpressing RTL1 are impaired in siRNA accumulation, but not in miRNA accumulation, leading to the conclusion that RTL1 degrades long, perfect, or near-perfect dsRNA substrates (Shamandi et al. 2015). Furthermore, viral infection induces RTL1 expression, and its RNase function can be disrupted by viral suppressors of RNA silencing (Shamandi et al. 2015). In contrast, RTL2 cleaves dsRNA substrates into smaller >25-nt-long dsRNA molecules, a function which can enhance or diminish the accumulation of different categories of PolIV and DCL3-dependent endogenous p4-siRNAs that impact genome methylation (Comella et al. 2008; Elvira-Matelot et al. 2016). It has not been reported whether RTL functions are impacted in any manner by DRB proteins.

A recent phylogenetic analysis of DRBs in plants (Clavel et al. 2016) identified a new clade of DRB protein, DRB7, conserved in all vascular plants, with only one dsRBM that shares closest sequence identity with the second dsRBM of DCL4. This gene family is represented by *DRB7.1* and *DRB7.2* in *Arabidopsis*. DRB7.2 interacts with DRB4, but not with DCL4, and *drb7.2* mutation selectively impairs the processing of endogenous inverted repeat dsRNA into siRNAs through direct binding of the substrate (Montavon et al. 2016) and also impacts the accumulation pattern of epigenetically activated (ea)siRNAs when combined with a mutation in *decreased DNA methylation 1* (*ddm1*). The other member of the *DRB7* family, *DRB7.1*, albeit similar to *DRB7.2*, has not been assigned any role in RNA silencing pathways and its function remains elusive. (Clavel et al. 2016).

Many fundamental insights about plant ribonuclease and RNA binding protein functions were first established through in vitro studies. *Nicotiana tabacum* cultivar Bright Yellow-2 evacuolated lysate (BYL), an equivalent to *Drosophila* embryo extract (Lakatos et al. 2006), has emerged as an efficient and biologically relevant in vitro system for the analysis of RNA metabolism, RNA silencing (Iki et al. 2010, 2012; Ye et al. 2012; Endo et al. 2013; Iwakawa and Tomari 2013; Yoshikawa et al. 2013), and virus infection (Komoda et al. 2004). We demonstrate here that BYL represents an informative in vitro system to study and characterize biochemical properties of a complex of proteins on the processing of various dsRNA substrates.

In this study, we report that DRB7.1 interacts with DRB4 in planta. We further show, using BYL in vitro assays, that DRB7.1 and DRB4 together can impair the processing of dsRNA substrates into siRNAs by RNase III-containing proteins. Using an in vivo approach with plants overexpressing DRB7.1, we observed alteration in the processing of small

TABLE 1. Peptide fingerprints identified by MS/MS specific to DCL4-FHA and DRB4-YFP-Flag immunoprecipitation samples

Batch no.	MS/MS view identified protein	Locus	Accession number	Molecular weight (kDa)	Exclusive unique peptide count	Percent coverage %
DCL4 IP.1	Dicer-like protein 4	At5g20320	sp | P84634 | DCL4_ARATH	191	92	50
	Double-stranded RNA-binding protein 4	At3g62800	sp | Q8H1D4 | DRB4_ARATH	38	19	76
DCL4 IP.2	Dicer-like protein 4	At5g20320	sp | P84634 | DCL4_ARATH	191	61	41
	Double-stranded RNA-binding protein 4	At3g62800	sp | Q8H1D4 | DRB4_ARATH	38	14	57
DCL4 IP.3	Dicer-like protein 4	At5g20320	sp | P84634 | DCL4_ARATH	191	37	26
	Double-stranded RNA-binding protein 4	At3g62800	sp | Q8H1D4 | DRB4_ARATH	38	6	29
DRB4 IP.1	Double-stranded RNA-binding protein 4	At3g62800	sp | Q8H1D4 | DRB4_ARATH	38	15	60
	Dicer-like protein 4	At5g20320	sp | P84634 | DCL4_ARATH	191	33	24
	Ribonuclease 3-like protein → DRB7.1	At1g80650	sp | Q9M8N2 | RTL1_ARATH	23	2	14
DRB4 IP.2	Double-stranded RNA-binding protein 4	At3g62800	sp | Q8H1D4 | DRB4_ARATH	38	11	37
	Dicer-like protein 4	At5g20320	sp | P84634 | DCL4_ARATH	191	18	12
	Ribonuclease 3-like protein → DRB7.1	At1g80650	sp | Q9M8N2 | RTL1_ARATH	23	1	3
DRB4 IP.3	Double-stranded RNA-binding protein 4	At3g62800	sp | Q8H1D4 | DRB4_ARATH	38	11	34
	Dicer-like protein 4	At5g20320	sp | P84634 | DCL4_ARATH	191	17	10
	Ribonuclease 3-like protein → DRB7.1	At1g80650	sp | Q9M8N2 | RTL1_ARATH	23	2	14

RNA species recapitulating a mild *drb4* mutant phenotype. Characterizing the DRB7.1–DRB4 interaction thus suggests two mechanisms whereby DRB7.1 can modulate small RNA biogenesis: (i) by direct binding of a dsRNA substrate in complex with DRB4 and (ii) by sequestering DRB4.

RESULTS

Identification of the DRB4 interactor DRB7.1

To discover new proteins that could regulate RNA silencing, we searched for interactors of DCL4 and DRB4. Transgenic *Arabidopsis* plants expressing native promoter-driven fusions of *Flag* and *HA* epitopes (*FHA*) with the *DCL4* genomic coding sequence, or a yellow fluorescent protein (*YFP*)-*Flag* epitope fusion to *DRB4*, were established in the *dcl4-2* and *drb4-1* mutant backgrounds, respectively. Immunoprecipitation was then performed with Flag antibodies using crude tissue extracts of transgenic plants, and with nontransgenic wild-type plants (Col-0 WT) as a negative control. Three independent immunoprecipitation experiments were performed, analyzed by liquid chromatography electrospray ionization coupled with tandem mass spectrometry (LC/ESI/MS/MS), and the resulting peptide spectra were compared against the Swiss-Prot database (Table 1). Only the proteins found in DCL4/DRB4 fractions, for which no peptides were found in Col-0 WT fractions (negative control), were considered as potential interactors. As expected, DRB4 was specifically identified in all DCL4-immunoprecipitated samples and DCL4 was identified in all DRB4-immunoprecipitated samples (Table 1). In addition, AT1G80650 was specifically identified in all DRB4 fractions, while DCL4 immunoprecipitation did not reveal any additional interactors. Online databases, such as Swiss-Prot, assign AT1G80650 the name RTL1; however, this gene encodes a dsRBM but does not encode a predictable RNase III domain (see Supplemental Fig. S1). A recent phylogenetic study renamed this protein DRB7.1 (double-stranded RNA binding protein 7.1) (Clavel et al. 2016), a nomenclature we adopt for its accuracy and to avoid confusion with the bona fide RNase III-containing RTL1 (AT4G15417) (Shamandi et al. 2015). Subsequent analysis of peptide fingerprints identified DRB7.2 as a specific interactor of DRB4 when compared against the TAIR10 protein database (data not shown), consistent with previous reports (Clavel et al. 2016; Montavon et al. 2016).

DRB7.1 interacts with DRB4 and indirectly with DCL4

To confirm the interaction between DRB7.1 and DRB4 we performed a Bimolecular Fluorescence Complementation assay (BiFC) (Bracha-Drori et al. 2004) by transient expression in *Nicotiana benthamiana* leaves. In this experiment, proteins of interest are coexpressed as fusions to YFP halves, and a fluorescent signal is only produced when the two proteins interact and reconstitute an active fluorophore. The known interaction between DRB4 and DCL4 was used as a positive control (Nakazawa et al. 2007; Clavel et al. 2016), resulting in fluorescence complementation observed by confocal microscopy in a distinctive punctate pattern in nuclei of cells coexpressing DRB4 and DCL4 fused to YFP halves (Fig. 1A). Coexpression of DRB7.1 and DRB4 fused to YFP halves consistently produced fluorescent signals localized in nuclear punctae (Fig. 1B), similar to those observed between DRB4

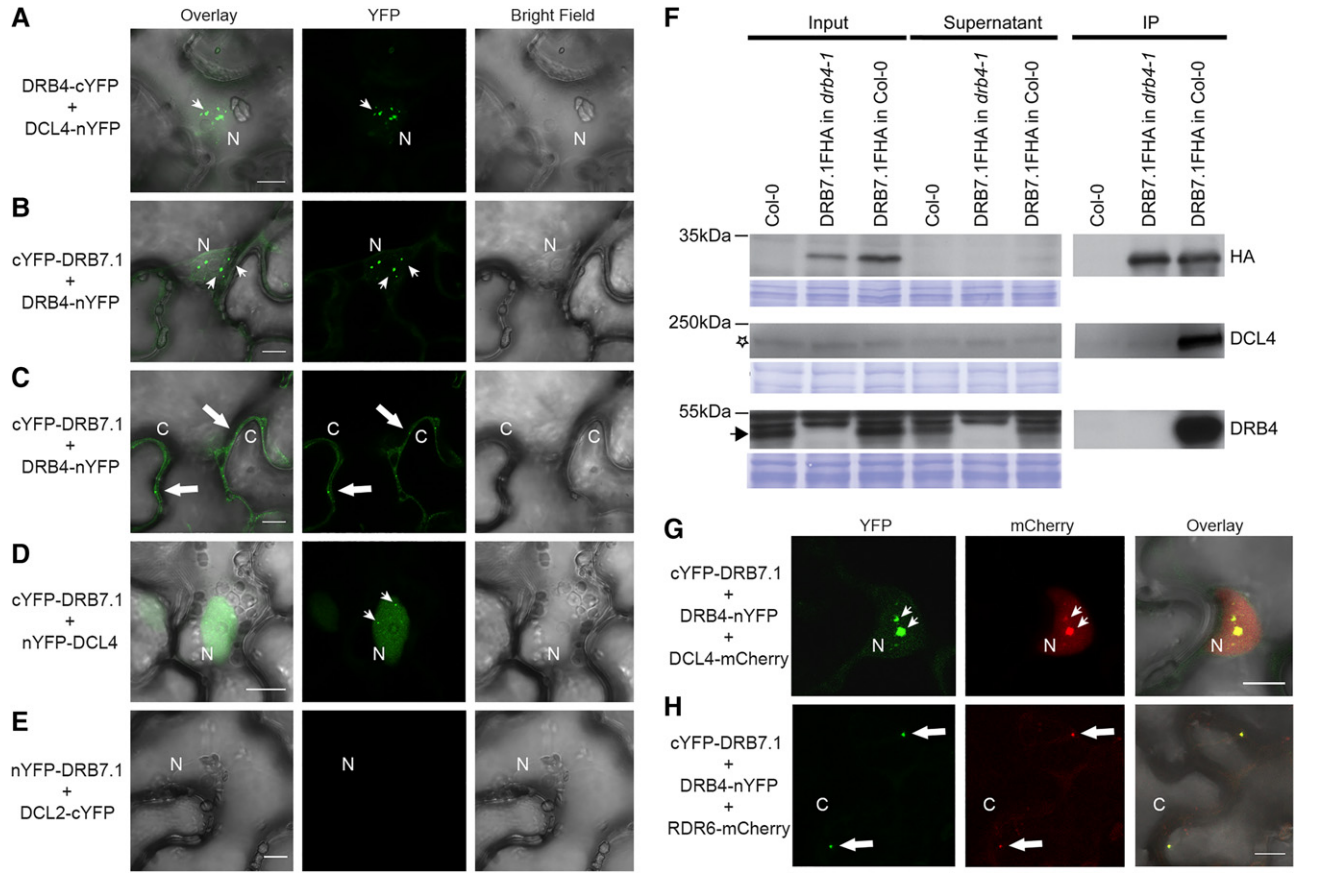

FIGURE 1. DRB7.1 interacts with DRB4 and DCL4. (*A–E*) Bimolecular fluorescence complementation assay (BiFC) performed by transient expression in *N. benthamiana* leaves and imaged by confocal microscopy. YFP signal emitted from reconstituted half-YFP fusions to the proteins indicated on panels is shown together with bright-field (differential interference contrast) and an overlay of channels. (*F*) Western blot analysis of DRB7.1: DRB7.1-FHA following immunoprecipitation with anti-Flag antibodies from WT Col-0 or *drb4-1* mutant plants. Immunoprecipitated DRB7.1 fusion protein is detected with an HA antibody, and coimmunoprecipitated DCL4 and DRB4 are detected by native antibodies. Total protein staining by Coomassie blue is shown as a loading control for input and supernatant (unbound fraction). Star indicates background band that cross-reacts with DCL4 antibody. Arrow indicates DRB4 band, to distinguish from background cross-reacting bands. (*G*,*H*) Colocalization of YFP signals from DRB7.1+DRB4 BiFC with DCL4-mCherry (*G*) and RDR6-mCherry (*H*) performed by transient expression in *N. benthamiana* leaves and imaged by confocal microscopy. Nucleus (N) and cytoplasm (C) are indicated. Arrowheads indicate nuclear foci, arrows indicate punctate cytoplasmic signals. Scale bar = 10 μm.

and DCL4, but also in cytoplasmic punctae (Fig. 1C, which shows a different focal plane along the *z*-axis of the same sample shown in Fig. 1B). Coexpressing DRB7.1 and DCL4 fusions also yielded fluorescent punctae in nuclei (Fig. 1D), demonstrating that these proteins interact under BiFC experimental conditions. This pattern was different from that observed with DRB7.1 and DRB4, because in addition to nuclear punctae, DRB7.1 and DCL4 also displayed a diffuse signal throughout the nucleoplasm, while no cytoplasmic signals were observed (Fig. 1D). In contrast, coexpressing DRB7.1 and DCL2 fusions did not result in fluorescence complementation (Fig. 1E). This result serves as a negative control and demonstrates the specificity of DRB7.1 interaction with DCL4 and DRB4.

To further confirm these interactions, we established transgenic plants expressing an *FHA* fusion to *DRB7.1* driven from its native promoter (*DRB7.1:DRB7.1-FHA*). The tagged protein was immunoprecipitated with anti-Flag antibodies from crude inflorescence extracts and analyzed by Western blotting to test for coimmunoprecipitation of endogenous DRB4 and DCL4 proteins. In wild-type plants, both endogenous DRB4 and DCL4 were coimmunopurified with DRB7.1-FHA (Fig. 1F), further confirming the interactions observed by mass spectrometry and BiFC. To test if the interaction between DRB7.1 and DCL4 is dependent on the presence of DRB4, immunoprecipitation experiments were repeated using *drb4-1* mutant plants expressing *DRB7.1: DRB7.1-FHA*. Interestingly, in *drb4-1* plants, DCL4 did not coimmunoprecipitate with DRB7.1-FHA (Fig. 1F), suggesting that the interaction between DRB7.1 and endogenous DCL4 is dependent on DRB4 in *Arabidopsis*. Together, these results demonstrate that DRB7.1 is a robust interactor of DRB4 and that DRB7.1 likely interacts indirectly with DCL4 via a DRB4 "bridge." In this case, the BiFC interaction can

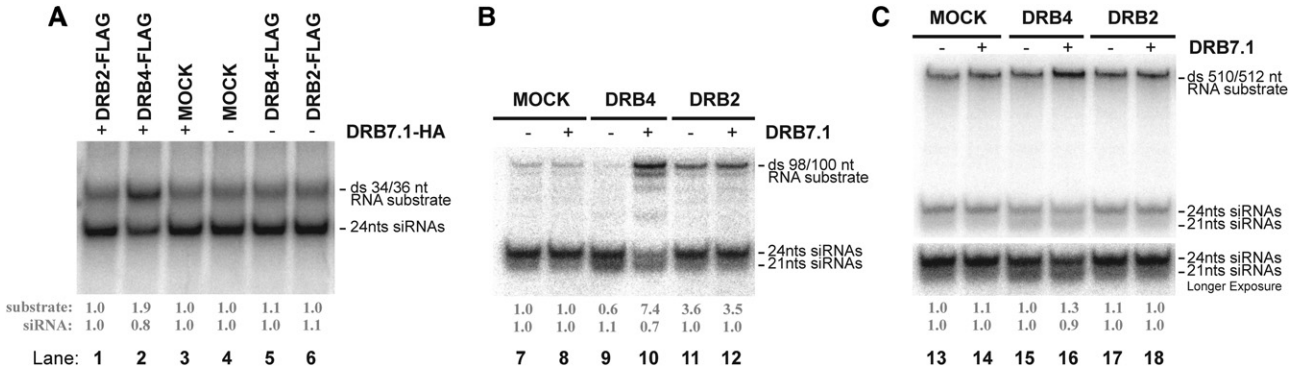

FIGURE 2. Combining DRB7.1 with DRB4 in BYL impairs endogenous dsRNA processing. (*A–C*) DRB7.1, DRB7.1-HA, DRB4, DRB4-Flag, DRB2, and DRB2-Flag were in vitro translated in BYL, mixed together and incubated for 15 min with 34/36-nt (*A*), or 30 min with 98/100-nt (*B*), and 510/512-nt (*C*) radiolabeled dsRNA substrates. RNA was extracted and separated on 15% native polyacrylamide gel. MOCK samples (lysate with no addition of exogenous mRNA) represent the endogenous processing activity of the lysate after addition of radiolabeled dsRNA and is used as a baseline control. Normalized quantification of band intensity is displayed *below* the gel. Substrates and siRNAs intensity values were normalized to Mock values.

be explained by endogenous DRB4 from *N. benthamiana* bridging the DRB7.1–DCL4 fluorescence complementation.

The interaction between DRB7.1 and DRB4 colocalizes with markers of siRNA- and dicing bodies

To characterize the discrete punctate localization of the DRB7.1 and DRB4 interaction observed by BiFC, we performed colocalization by transient expression in *N. benthamiana*. BiFC was performed together with markers of nuclear DCL4^{NLS}-mCherry, which forms nuclear dicing bodies together with DRB4 (Pumplin et al. 2016) and RDR6-mCherry, which localizes in cytoplasmic siRNA bodies that are the likely source of dsRNA used to amplify the PTGS pathway (Kumakura et al. 2009; Jouannet et al. 2012). The BiFC signal between DRB7.1 and DRB4 indeed colocalized in nuclear dicing bodies with DCL4 (Fig. 1G). Interestingly, the DRB7.1–DRB4 interaction also dynamically colocalized in the cytoplasm with RDR6-mCherry (Fig. 1H; Supplemental Movie S1, S2). These results demonstrate that DRB7.1 and DRB4 interact in sites likely to be enriched in dsRNA, and may function in the siRNA-generating pathway.

DRB7.1 impairs in vitro dicing in a DRB4-dependent manner

To characterize the biochemical function of DRB7.1 in relation to siRNA processing involving DRB4, we used the BYL in vitro system, which allows the efficient characterization of protein overexpression on endogenous RNA processing activities. Similar to *Arabidopsis* cell extracts, (Qi et al. 2005; Fukudome et al. 2011; Nagano et al. 2014), BYL processes dsRNA mainly into 24- and 21-nt siRNAs (Fig. 2A–C, MOCK –, lanes 4,7,13, and Iki et al. 2017), most likely relying on endogenous DCL3 and DCL4 activities, respectively. DRB7.1, DRB4, as well as DRB2 used for comparison, were individually expressed in BYL by addition of corresponding in vitro-transcribed mRNAs (see Supplemental Fig. S2 for experimental outline). Lysates containing the indicated proteins as well as the MOCK sample, corresponding to the lysate with no addition of exogenous mRNA, were incubated together with exogenous radiolabeled artificial dsRNAs of 34 base pairs (bp) (34/36-nt duplex), 98 bp (98/100-nt duplex), or 510 bp (510/512-nt duplex), each containing one blunt end and one 2-nt 3′ overhang.

Addition of dsRNA of all three sizes to DRB7.1-expressing BYL did not alter the small RNA accumulation pattern relative to the MOCK control sample (Fig. 2A–C, cf. lane 3 to 4, lane 8 to 7, and lane 14 to 13), suggesting that DRB7.1 alone had no influence on endogenous processing activity. Incubation of DRB4-expressing BYL with 98- and 510-bp substrates caused increased accumulation of 21-nt siRNAs, owing to the function of DRB4 to promote DCL4 activity (Fig. 2B, cf. lane 9 to 7 and Fig. 2C, cf. lane 15 to 13). This result is consistent with previous BYL experiments (Iki et al. 2017) and also in vitro experiments showing that DRB4 facilitates DCL4 processing of longer dsRNA substrates (Fukudome et al. 2011). Notably, DRB4 expression did not lead to accumulation of 21-nt siRNAs from the 34-bp substrate, which only produces detectable 24-nt siRNAs in BYL (Fig. 2A, cf. lane 5 to 4). This result is consistent with previous work showing that DCL4 does not process dsRNA of 30 bp and only inefficiently processes 37-bp dsRNA (Nagano et al. 2014).

Remarkably, incubation of dsRNA with a mixture of DRB7.1- and DRB4-expressing BYL consistently led to a decreased accumulation of 24-nt siRNAs and a corresponding increased accumulation of unprocessed longer dsRNA for all three lengths of substrate (Fig. 2A–C, cf. lane 2 to 4, lane 10 to 7, and lane 16 to 13). These results suggest that the DRB7.1/DRB4 complex can impair dicing, while neither

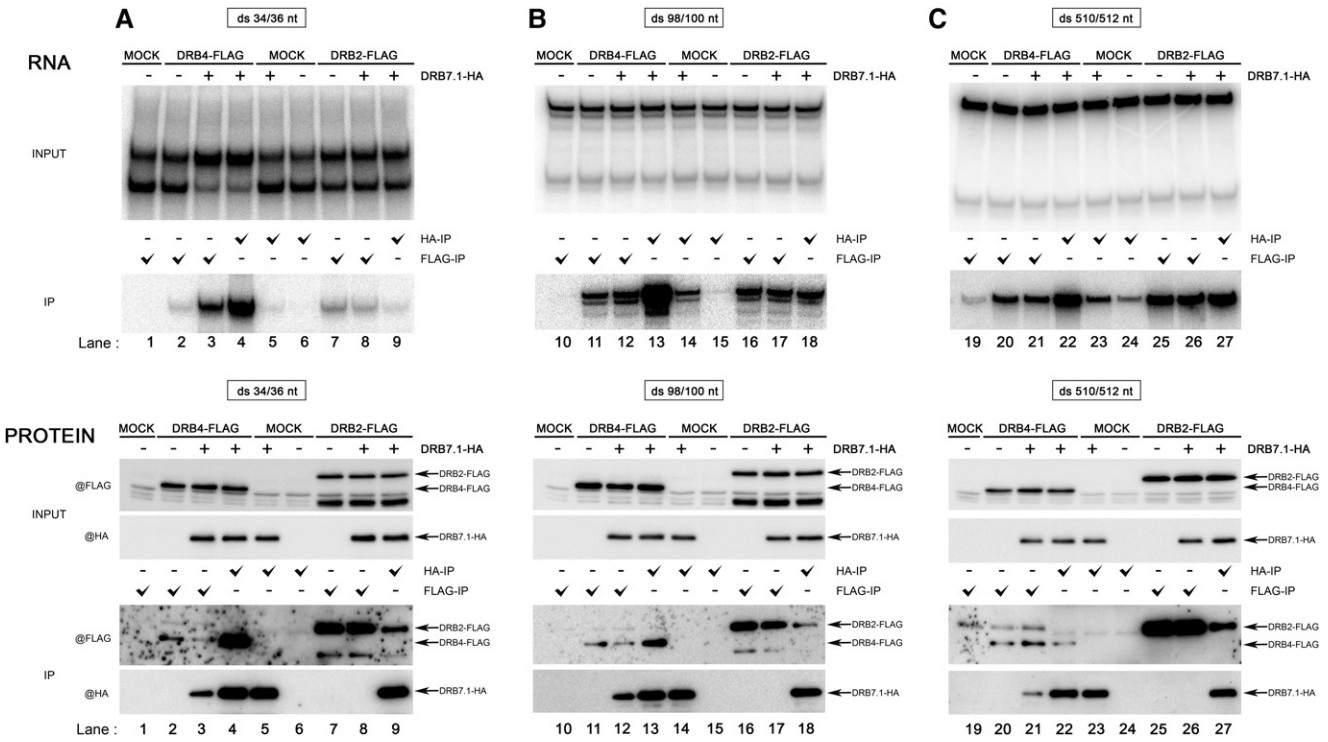

FIGURE 3. Coimmunopurification of dsRNA with DRB7.1, DRB4, and DRB2. (*A–C*) DRB7.1-HA, DRB4-Flag, and DRB2-Flag were in vitro translated in BYL and combined as indicated (protein input, *bottom*), then incubated with radiolabeled dsRNA substrates of various sizes. After 7 min of incubation, RNA input (*top*) was extracted. For immunoprecipitation (IP), Flag or HA magnetic beads were added to the BYL mixes and incubated for 40 min at 4°C, followed by washes. A fraction of magnetic beads was used for protein extraction (protein IP, *bottom*) and RNA was extracted from the remaining sample (RNA IP, *top*). RNA was separated on 15% native polyacrylamide gel. Proteins were resolved on 12% SDS–PAGE gel.

DRB7.1 nor DRB4 alone impaired processing activity. Furthermore, the combination of BYL expressing DRB7.1 and DRB4 did not lead to an increased accumulation of 21-nt siRNAs from the 98-bp dsRNA (Fig. 2B, lane 10) as observed for DRB4 alone (Fig. 2B, lane 9), suggesting that DRB7.1 negates the DCL4-stimulating activity of DRB4. DRB2-expressing BYL alone displayed a minor effect of stabilizing 98-bp substrates, but did not impact processing of 510- or 34-bp substrates (Fig. 2A–C, cf. lane 6 to 4, lane 11 to 7, and lane 17 to 13). Furthermore, combining DRB2 and DRB7.1 in BYL did not display differing activities relative to DRB2 alone (Fig. 2A–C, cf. lane 1 to lane 6, 12 to 11, and lane 18 to 17). Taken together, these results show that DRB7.1 can specifically function with DRB4 to impede production of 24-nt siRNAs and negate the increased production of 21-nt siRNAs.

DRB7.1 binds dsRNAs in BYL

Next, we examined the binding affinity of DRB7.1 and the complex formed by DRB7.1 and DRB4 to dsRNA substrates in BYL. DRB7.1-HA, DRB4-Flag, or DRB2-Flag fusion proteins overexpressed in BYL were immunoprecipitated with either Flag or HA antibodies following incubation with radiolabeled dsRNA substrates. RNA bound to DRBs was extracted directly after protein immunoprecipitation. These experiments were carried out after a shorter incubation with dsRNA relative to experiments shown in Figure 2, which minimized dsRNA processing and thus provided more equal inputs.

DRB7.1 coimmunopurified 98- and 510-bp dsRNA (Fig. 3B, cf. lane 14 to 15 and Fig. 3C, cf. lane 23 to 24), demonstrating that DRB7.1 is likely a bona fide RNA binding protein with higher affinity to longer dsRNA and weak but detectable affinity for 34-bp dsRNA (Fig. 3A, cf. lane 5 to 6). Immunopurified DRB4 demonstrated a pattern similar to DRB7.1 and previous reports (Hiraguri et al. 2005; Fukudome et al. 2011), with significant binding of 98- and 510-bp dsRNAs (Fig. 3B, cf. lane 11 to 10, and Fig. 3C, cf. lane 20 to 19) and weak binding of 34-bp dsRNA duplex (Fig. 3A, cf. lane 2 to 1).

Combining DRB7.1 with DRB4 greatly increased the amount of coprecipitated 34- and 98-bp dsRNA compared to the two proteins alone (Fig. 3A and B, cf. lanes 3 and 4 to lanes 2 and 5, and lanes 12 and 13 to lanes 11 and 14). Combining DRB7.1 and DRB4 with 510-bp dsRNA did not lead to enhanced coprecipitation of the substrate relative to DRB4 alone (Fig. 3C, cf. lane 21 to lane 20). This suggests that the DRB7.1/DRB4 complex, compared with each protein alone, has increased affinity for shorter dsRNA, but not for the

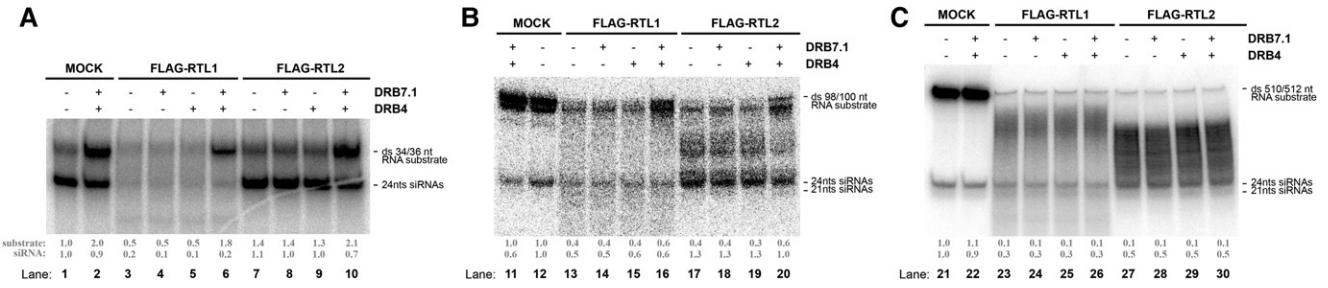

FIGURE 4. Combining DRB7.1 with DRB4 impairs dsRNA processing by RTL1 and RTL2 on shorter dsRNA substrates. (*A–C*) DRB7.1, DRB4, Flag-RTL1, and Flag-RTL2 were in vitro translated in BYL, mixed together as indicated and incubated for 15 min (*A*), 30 min (*B*), or 20 min (*C*) with dsRNA substrates of indicated size. RNA was extracted and separated on 15% native polyacrylamide gel. MOCK (- -) samples (lanes *1*,*12*, and *21*) represent the endogenous processing activity of the lysate after addition of radiolabeled dsRNA and is used as a control for processing pattern. Flag-RTL1 (- -) or Flag-RTL2 (- -) are used as controls for respective RTL activity in this experiment. (*A*) DRB7.1 mixed with DRB4 impairs processing of 34/36 RNA duplexes by Flag-RTL1. Flag-RTL2 does not process 34/36 RNA duplexes. (*B*) DRB7.1 mixed with DRB4 impairs processing of 98/100 RNA duplexes by Flag-RTL1 and Flag-RTL2. (*C*) Combining DRB7.1 and DRB4 does not impede RTL1 and RTL2 dsRNA processing of 510/512 nt. Normalized quantification of band intensity is displayed *below* the gel. Substrates and siRNAs intensity values were normalized to Mock values.

510-bp dsRNA. It is important to note that the DRB7.1/DRB4 complex can impair dicing of the 510-bp substrate, while DRB4 alone does not (Fig. 2), suggesting that this activity is not solely due to binding affinity. In contrast, combining DRB7.1 with DRB2 did not enhance the affinity of DRB2 to bind dsRNA (Fig. 3A–C, cf. lanes 8,17,26 to 7,16,25).

Western blotting demonstrated equal levels of protein input, and also confirmed the interaction between DRB7.1 and DRB4 by reciprocal coimmunoprecipitation in BYL lysate (Fig. 3A–C). Protein analysis also revealed that the greater level of RNA coprecipitated by HA immunoprecipitation is not due to preferential RNA binding by DRB7.1, but rather due to enhanced antibody affinity (Fig. 3A, cf. lanes 3,4 and 11,12) as evidenced by the enhanced precipitation of DRB4-Flag by immunoprecipitation with HA (indirect via DRB7.1-HA, lanes 4,12) relative to Flag (direct, lanes 3,11). Coimmunoprecipitation of DRB2 was observed when DRB7.1 was immunoprecipitated, but not vice versa (Fig. 3A–C), suggesting that this interaction is significantly weaker than that of DRB7.1 and DRB4 or an artifact of the immunoprecipitation from BYL. Our results demonstrate that DRB7.1 can bind dsRNA and, taken together, show that DRB7.1 specifically partners with DRB4 and impacts siRNA processing by associating with dsRNA substrates in vitro.

DRB7.1 and DRB4 impair processing by RTL1 and RTL2

In addition to DCLs, plants also encode another class of RNase III proteins called RTLs. We thus tested whether the effect of DRB7.1 and DRB4 to impair dsRNA processing was specific to DCLs or was a more general mechanism that could additionally impair the RNase III activity of RTL1 and RTL2.

Incubation of Flag-RTL1-expressing BYL with 34- or 98-bp dsRNA substrates resulted in strongly decreased accumulation of both precursor and processed siRNAs compared to the MOCK control sample (Fig. 4A,B, cf. lane 3 to 1 and lane 13 to 12). This in vitro observation corroborates previously described effects of RTL1, which caused a strong reduction but not a complete loss of siRNAs when expressed in transgenic plants; moreover, fusing RTL1 to a Flag epitope was shown to reduce its activity (Shamandi et al. 2015). Combining either DRB7.1 or DRB4 with RTL1 did not impact its effect on dsRNA processing following addition of 34- or 98-bp dsRNA (Fig. 4A, cf. lanes 4,5 to lane 3 and Fig. 4B, cf. lanes 14,15 to lane 13). Remarkably, adding both DRB7.1 and DRB4 in combination with RTL1 led to a stabilization of the unprocessed substrate, showing that the DRB7.1/DRB4 complex is able to impair RTL1 action on dsRNA (Fig. 4A, cf. lane 6 to lane 3 and Fig. 4B, cf. lane 16 to 13). This stabilization did not correlate with an increase in DCL-dependent siRNAs, suggesting that the portion of dsRNA bound by DRB7.1/DRB4 does not become available to the DCL activity of BYL, as shown in Figure 2.

In contrast to RTL1, incubation of RTL2-expressing BYL with 98-bp dsRNA led to the accumulation of multiple intermediate-sized dsRNA not detected in the MOCK control, and increased accumulation of 24-nt siRNAs (Fig. 4B, cf. lane 17 to 12), consistent with the RTL2 function demonstrated by in vivo and in vitro assays (Comella et al. 2008; Elvira-Matelot et al. 2016). Combining either DRB7.1 or DRB4 with RTL2 had no effect on RTL2 processing (Fig. 4B, cf. lanes 18,19 to lane 17). However, when RTL2 was combined with both DRB7.1 and DRB4, we observed an increased accumulation of unprocessed dsRNA substrate and a reduction in the accumulation of the intermediate-sized products as well as a reduction of 24-nt small RNAs (Fig. 4B, cf. lane 20 to lane 17). These results show that the complex formed by DRB4 and DRB7.1 interferes with RTL2 activity on dsRNA. Notably, RTL2 did not affect stability or dicing of the 34-bp dsRNA substrates (Fig. 4A, cf. lane 7 to lane 1), nor did RTL2 impact the ability of the DRB7.1/DRB4 complex to impair dicing (Fig. 4A, cf. lane 10 to lane 2). Interestingly, addition of both DRB7.1 and DRB4 with either RTL1 or RTL2 did not impair processing of the 510-bp dsRNA substrate (Fig.

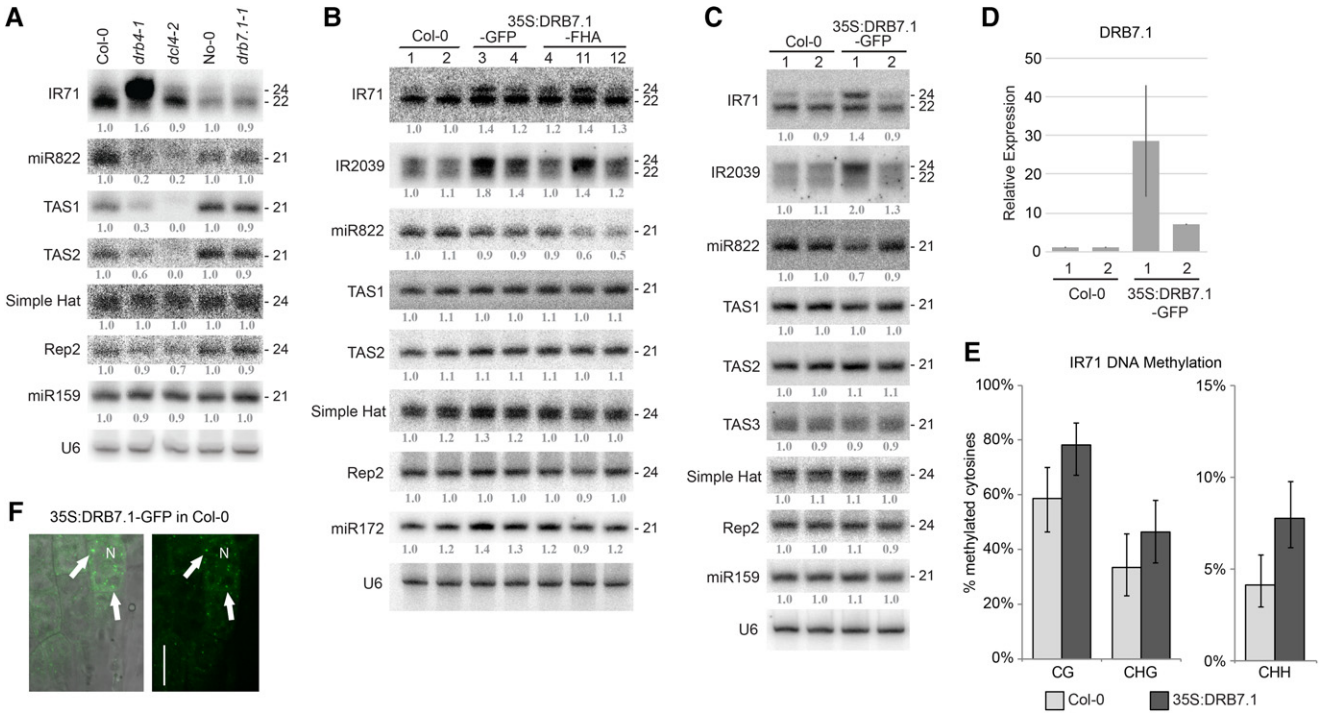

FIGURE 5. Effect of *drb7.1-1* and DRB7.1 overexpression on siRNA accumulation. (*A*) Low-molecular weight RNA blot with RNA extracted from inflorescences of *drb7.1-1* and No-0 control, and *dcl4-2*, *drb4-1*, and Col-0 control. DCL2/DCL3-dependent IR71, DCL4-dependent miR822, TAS1 and 2, DCL3-dependent SimpleHat and Rep2, and DCL1-dependent miR159 are shown. (*B*) Low-molecular weight Northern blotting was performed on total RNA extracted from inflorescences of independent, stable transgenic Col-0 WT plants expressing 35S:DRB7.1-GFP or 35S:DRB7.1-FHA. Two independent samples from Col-0 WT control plants are included. DCL2/DCL3-dependent IR71 and IR2039, DCL4-dependent miR822, TAS1 and 2, DCL3-dependent SimpleHat and Rep2, and DCL1-dependent miR172 are shown. (*C*) Similar analysis as *B*, but performed with batches of T1 plants and with addition of DCL4-dependent TAS3. (*A–C*) U6 is included as a loading control. siRNA sizes are indicated. The same Northern blot membrane was stripped and rehybridized with different probes to analyze multiple siRNA species. Normalized quantification of band intensity is displayed *below* the gel image. Intensity values were normalized to U6 and are displayed as a ratio relative to Col-0 (wild-type) sample. (*D*) Relative expression of DRB7.1, measured by RT-qPCR, of T1 pools. Average of two biological replicates (batches) ± standard deviation is shown. (*E*) Bisulfite sequencing PCR (BSP) analysis of *IR71 5′* region in all contexts (CG, CHG, and CHH sites) in WT (Col-0) and DRB7.1 OX lines. Error bars represent 95% confidence intervals, calculated using Wilson score interval. (*F*) Confocal image of 35S:DRB7.1-GFP localization in a live root of Col-0 WT background. Arrow, cytoplasmic punctae; N, nucleus. Scale bar = 10 µm.

4C), suggesting that the relative activity of RTL1 and RTL2 on long dsRNA may be higher than that of the DRB7.1/DRB4 complex, and also that this complex does not directly impair RTL enzymatic activity. These results show that in BYL, DRB7.1, and DRB4 together, but not individually, can impair dsRNA processing by RTL1 and RTL2, suggesting a general antagonistic function toward RNase III enzymes.

DRB7.1 is not required for siRNA accumulation in whole tissues

To analyze the biological role played by DRB7.1 and its potential to modulate dsRNA processing in vivo, we set out to characterize *drb7.1* mutant plants. No *drb7.1* mutants were available in the reference ecotype Colombia (Col-0), but an insertional mutant harboring a transposon in the third exon of *DRB7.1* is available in the Nossen (No-0) ecotype (Supplemental Fig. S1A). Real-time quantitative PCR (RT-qPCR) analysis showed that *drb7.1-1* is a full knockout allele (Supplemental Fig. S3A). *drb7.1-1* mutants did not present any overt morphological phenotypes and developed similarly to No-0 WT plants (Supplemental Fig. S3B). Northern blotting analysis of RNA extracted from *drb7.1-1* and No-0 WT inflorescence samples revealed comparable siRNA accumulation patterns from all endogenous inverted repeats (IRs), tasiRNAs, DCL4-, and DCL1-dependent miRNAs, and DCL3-dependent siRNAs analyzed (Fig. 5A). This result, consistent with a recent report (Clavel et al. 2016), shows that loss of *DRB7.1* does not alter small RNA accumulation. In contrast, *drb4* mutant inflorescence samples accumulated less DCL4-dependent tasiRNAs and miR822, while they overaccumulated DCL3-dependent 24-nt siRNAs from *IR71* relative to the respective Col-0 WT control (Fig. 5A) as previously reported (Pelissier et al. 2011).

DRB7.1 overexpression impacts accumulation of certain siRNA species

As *drb7.1-1* mutant plants did not display a measurable phenotype, we asked if overexpression of DRB7.1 could impact

the RNA silencing pathway. Thus, *DRB7.1* genomic sequence fusions to green fluorescent protein (*GFP*) or *FHA* were overexpressed from the constitutive *Cauliflower mosaic virus* 35S promoter in the background of Col-0 WT plants. Inflorescences of independent T2 lines were analyzed by Northern blotting for effects on siRNA production. The overexpression lines displayed a subtle yet consistent reduction in the accumulation of the DCL4-dependent miR822 (Fig. 5B), suggesting an impairment of dsRNA processing. These lines also showed an increase in DCL3-dependent 24-nt siRNAs arising from inverted repeats IR71 and IR2039 (Fig. 5B), similar to the effect observed in *drb4* mutants (Fig. 5A). Because no changes to tasiRNAs were observed, this pattern resembles a mild *drb4* mutant phenotype and suggests that DRB7.1 may partially sequester DRB4. Accumulation of the subset of DCL3-dependent siRNAs tested was not impacted, contrasting with in vitro results when DRB7.1 and DRB4 were overexpressed together, but consistent with in vitro overexpression of DRB7.1 alone.

Because the overexpressing lines displayed heterogeneous effects on siRNA accumulation in different plants, we tested if these effects might depend on *DRB7.1* expression levels. Inflorescence populations from various pools of T1 plants expressing contrasting levels of *DRB7.1-GFP* were analyzed. The batch of T1 plants expressing low levels of *DRB7.1* (batch 2) did not alter siRNA accumulation relative to the WT control, while inflorescences from the higher-expressing T1 batch (batch 1) displayed impaired accumulation of DCL4-dependent miR822 and enhanced accumulation of DCL3-dependent 24-nt siRNAs from *IR71* and *IR2039* (Fig. 5C,D). This demonstrates that impairment of DRB4 function by DRB7.1 occurs in a dose-dependent manner.

The enhanced accumulation of 24-nt siRNAs from endogenous inverted repeat sequences represents an interesting result, as these DCL3-dependent species guide the RNA-directed DNA methylation (RdDM) pathway (Law and Jacobsen 2010; Matzke et al. 2014). This prompted us to explore whether DRB7.1 overexpression can influence genome methylation. We performed bisulfite sequencing to assay whether DNA methylation state changes at the IR71 locus would result from the increase in 24-nt siRNAs derived from this region. Interestingly, plants overexpressing DRB7.1 exhibited a significantly enhanced methylation level in the CHH context relative to the WT Col-0 control (Fig. 5E; Supplemental Fig. S4; Supplemental Table T3), suggesting that DRB7.1 has the capacity to play a biological role in the DNA methylation pathway.

Furthermore, confocal microscope imaging of roots from WT plants overexpressing DRB7.1-GFP revealed a signal in abundant cytoplasmic bodies (Fig. 5F). This localization pattern is similar to the DRB4-dependent siRNA body localization of DRB7.1 expressed from the native promoter and of the DRB4 + DRB7.1 interaction (Figs. 1C,H, 5). These cytoplasmic siRNA bodies could thus represent sites where DRB4 is sequestered from its role in the siRNA generation pathway, which likely occurs in the nucleus. These in vivo results show that overexpressed DRB7.1 causes a dosage-dependent mild *drb4* knockdown phenotype and correlates with changes in DNA methylation.

DRB7.1 is expressed in a restricted pattern

Because *DRB7.1* is not included in the widely used *Arabidopsis* ATH1 GeneChip, its expression was not characterized in the multitude of genome-wide studies characterizing tissue-specific transcript expression during growth and development. We thus investigated the DRB7.1 protein expression pattern and localization in *Arabidopsis* using a genomic coding sequence translational fusion of *DRB7.1* to *GFP* under the control of the native *DRB7.1* promoter (*DRB7.1:DRB7.1-GFP*). Col-0 WT plants were transformed with the fusion construct and the localization of DRB7.1-GFP in flowers, leaves, and roots was analyzed by epifluorescence and confocal microscopy.

A GFP signal was consistently detected only in floral meristems and in cells of the root cap of multiple plant lines (Fig. 6A; Supplemental Fig. S5A), but we were unable to detect GFP signal in the outer leaf cell layers (data not shown).

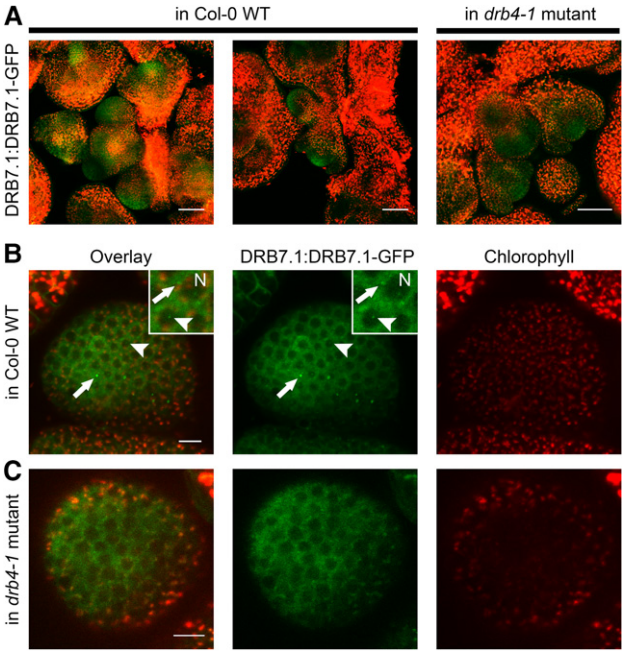

FIGURE 6. Expression pattern and localization of DRB7.1-GFP. (*A*) Confocal microscope images from a single plane of inflorescence meristems from DRB7.1:DRB7.1-GFP expressing Col-0 WT plants (*left* and *middle*) or a *drb4-1* mutant plant (*right*). Images depict GFP signal overlaid with chlorophyll autofluorescence. Scale bar = 50 µm. (*B*,*C*) Close-up images of a single plane from inflorescence meristems expressing the DRB7.1:DRB7.1-GFP fusion in Col-0 WT (*B*) or *drb4-1* mutants (*C*) with GFP signal (*middle*), chlorophyll autofluorescence (*right*) and overlay (*left*) shown. *Inset* depicts nucleus (N), nuclear foci (arrowhead), and cytoplasmic punctae (arrow). Scale bars = 10 µm.

For comparison, we also imaged inflorescences and roots of *DRB4:DRB4-YFP-Flag* reporter lines. DRB4-YFP localized in the same tissues as DRB7.1-GFP, but in contrast it was expressed additionally in a broad pattern in inflorescences, including tissues surrounding meristems and broadly in root tips (Supplemental Fig. S5B). The restricted expression domain of DRB7.1-GFP in limited cells of inflorescence meristems and root tips may therefore explain the lack of phenotype observed in *drb7.1-1* plants. Indeed, if *DRB7.1* contributes to siRNA production only in these cells, an effect could be diluted by the surrounding tissue and masked in whole-tissue analyses.

Punctate localization of DRB7.1 requires DRB4

In both inflorescences and roots of WT reporter plants, DRB7.1-GFP displayed a diffuse signal in the cytoplasm with an additional bright punctate signal in the cytoplasm (arrows) and in the nucleus (arrowheads) of a subset of cells (Fig. 6B; Supplemental Fig. S5A). This observation is consistent with BiFC localization showing an interaction between DRB4 and DRB7.1 in nuclear dicing bodies and cytoplasmic siRNA bodies (Fig. 1B,C,G,H).

To investigate whether DRB4 plays a role in DRB7.1 localization, *DRB7.1:DRB7.1-GFP* was transformed into *drb4-1* mutant plants. Intriguingly, the nuclear and cytoplasmic punctate pattern was lost when DRB7.1-GFP was observed in two independent *drb4* mutant transgenic plant lines, although the tissue-specific pattern of diffuse cytoplasmic signal remained the same as in WT plants (Fig. 6B,C; Supplemental Fig. S5C). To further test whether loss of DRB4 eliminated DRB7.1-GFP foci, we analyzed multiple, independent T1 transgenic plants by microscopy and compared expression levels of DRB7.1-GFP by Western blotting. This approach revealed that despite varying expression levels in both backgrounds, all WT plants displayed DRB7.1-GFP punctae, while no punctae could be observed in *drb4-1* mutants (Supplemental Fig. S6A,B). As a final confirmation, a stable transgenic *DRB7.1-GFP drb4-1* mutant plant was backcrossed to Col-0 WT. In the F1 of this cross, DRB7.1 punctae were restored coincidently to the addition of a WT *DRB4* allele (Supplemental Fig. S5C). These results reveal the requirement of DRB4 to specify DRB7.1-GFP localization in a punctate pattern and highlight that the interaction has a structural relevance in *Arabidopsis*.

DISCUSSION

Our study characterizes DRB7.1, a dsRNA binding protein that interacts with DRB4, and the implication of this protein complex in the small RNA biogenesis pathway. Multiple lines of evidence presented in this work suggest that DRB7.1 functions to antagonize dsRNA processing by RNase III enzymes via two mechanisms: by direct dsRNA binding in complex with DRB4, and by impairing the ability of DRB4 to function in siRNA biogenesis pathways through sequestration.

In vitro results suggest an antagonistic mechanism, whereby formation of a heteromeric DRB complex protects dsRNA from being processed by DCLs. This is highlighted in particular by the 34-bp dsRNA, which was strongly bound by DRB7.1/DRB4 together but not by each protein individually (Fig. 3A, lanes 2–5), and corresponds to the length of DCL3 substrates in vivo. Notably, DRB4 bound similar amounts of 510-bp dsRNA with or without DRB7.1 (Fig. 3C, lanes 20 and 21), suggesting that the protective effect of the two-protein complex cannot simply be explained by dsRNA binding affinity, but likely requires the assembled complex to prevent DCLs from accessing dsRNA. This explanation is further supported by the observation that DRB2 bound similar levels of 510-bp dsRNA as DRB7.1/DRB4, but did not impair dicing (Fig. 3C, lanes 21 and 26). In addition to impairing production of 24-nt siRNAs by DCL3, DRB7.1 also impaired the ability of DRB4 to promote DCL4 activity. The effect of DRB4 in enhancing production of 21-nt siRNAs from 98- and 510-bp dsRNA was lost when DRB7.1 was combined, suggesting that the DRB7.1/DRB4 complex does not promote DCL4-mediated siRNA biogenesis but instead functions as a repressive complex.

Because *drb7.1* mutant plants did not show detectable changes in siRNA production or phenotypes connected to altered RNA silencing, this gene does not serve an essential role in gene silencing in planta. It remains possible that *DRB7.1* may play a repressive role on dicing in a subset of cells within the plant, in which case we propose that its restricted expression domain in inflorescence meristems and root caps limits experimental observation of cell-specific siRNA production effects. For example, if 24- and 21-nt siRNAs are slightly increased in a few cells of the *drb7.1* mutant, this difference would not be observed by analyzing whole tissues due to dilution by the majority of cells, which never express *DRB7.1*. Overexpression of DRB7.1, meanwhile, mimicked a mild *drb4* mutant phenotype, suggesting that DRB4 could be partially sequestered from its role in producing miR822 small RNAs and inhibiting biogenesis of 24-nt siRNAs from inverted repeat dsRNA. This finding is consistent with in vitro BYL results that DRB7.1 prevents DRB4 from enhancing production of 21-nt siRNAs. Thus, in addition to dsRNA binding in complex with DRB4, DRB7.1 could impact the silencing pathway by modulating the amount of DRB4 available to function in the DCL pathway. Furthermore, the enhanced accumulation of DCL3-dependent 24-nt siRNAs derived from the endogenous inverted repeat observed in DRB7.1 overexpressing lines correlated with increased DNA methylation levels in the CHH context at the *IR71* locus (Fig. 5E). Thus the alterations to siRNA accumulation patterns mediated by DRB7.1 can exert downstream impacts on epigenetic marks, which could function

to fine-tune responses to environmental stresses (Matzke et al. 2014).

While DRB proteins are generally viewed as cofactors of DCLs that function to promote or facilitate robust dicing of small RNAs, our conclusion about DRB7.1 acting as an antagonist in the silencing pathway has precedent. For example, in an analogous pathway from animals, the dsRNA binding protein PACT impairs the activity of human Dicer to process pre-siRNAs (Lee et al. 2013). In plants, *drb4* and *drb7.2* mutants overaccumulate 24-nt siRNAs from inverted repeats because the DRB7.2 protein interacts with DRB4 and sequesters inverted repeat dsRNA, thus impairing its dicing by DCL3 (Pelissier et al. 2011; Montavon et al. 2016). DRB7.1 overexpression therefore represses the repressive function of DRB4, indirectly leading to an increase in 24-nt siRNAs from inverted repeats. Meanwhile *drb2* mutant plants overaccumulate DCL3-dependent p4-siRNAs, which guide DNA methylation, while DRB2 overexpression can impair the accumulation of p4-siRNAs (Pelissier et al. 2011). Furthermore, DRB2 overexpression antagonizes the DRB4 pathway through an unknown mechanism, resulting in a reduced accumulation of tasiRNAs and a leaf morphology phenotype that mimicked *drb4* mutants (Pelissier et al. 2011). Intriguingly, *drb2* mutation showed reduced accumulation of miR822 (Pelissier et al. 2011), suggesting that while DRB7.1 impaired miR822 production, DRB2 promotes its biogenesis. Finally, *drb7.2 ddm1* and *drb4 ddm1* double mutants led to increased production of 24-nt epigenetically activated (ea) siRNAs, which are otherwise predominantly 21-nt-long and DCL4-dependent in *ddm1* single mutants (Creasey et al. 2014; Clavel et al. 2016); thus DRB4 and DRB7.2 can repress production of 24-nt easiRNA species in a similar manner to 24-nt inverted repeat siRNA species. Nonetheless, a major function of DRB2 and DRB4 is clearly in promoting biogenesis of small RNAs (Adenot et al. 2006; Pelissier et al. 2011; Eamens et al. 2012a; Reis et al. 2015). In contrast, no experiments revealed a role for DRB7.1 or DRB7.2 in directly promoting the biogenesis of any small RNA, including small RNA sequencing performed on *drb7.2* mutants (Montavon et al. 2016). Thus, this clade of DRBs may have evolved to exert a purely repressive function, both on dsRNA processing and on the function of DRB4. It should be noted here that DRB3 and DRB5 do not appear to function in small RNA biogenesis, and thus additionally function outside of the standard paradigm of DRB proteins as DCL accessories (Eamens et al. 2012b; Raja et al. 2014).

Comparing our results with *DRB7.1* mutation and overexpression to previous characterization of *drb7.2* and *drb7.1* (Clavel et al. 2016; Montavon et al. 2016) reveals that *DRB7.1* and *DRB7.2*, although closely related, are not functionally redundant. In addition to their opposite effects on siRNA production from inverted repeats noted above, it has been previously shown using an inter-ecotype genetic cross that the double *drb7.1 drb7.2* mutant had no impact on the accumulation of a certain subset of DRB4 and DCL4-dependent siRNAs tested (Clavel et al. 2016). Furthermore, DRB7.2 localizes in the nucleus and DRB4 interacts with DRB7.2 or DCL4 in a mutually exclusive manner (Montavon et al. 2016). In contrast, DRB7.1 can interact simultaneously with DRB4 and DCL4, and localizes mainly in the cytoplasm in a punctate pattern that colocalized with the siRNA body marker RDR6 in heterologous expression experiments. Thus, investigating the structural basis guiding the differing properties between DRB7.1 and DRB7.2 would be particularly informative.

While DRB proteins are well known to function in the DCL pathway, they have not been studied in the context of different classes of RNase III enzymes. Here, we could recapitulate RTL1- and RTL2-dependent dsRNA degradation effects in the BYL system (Shamandi et al. 2015; Elvira-Matelot et al. 2016). We report that RTL2 has no effect on the processing of 34-bp dsRNA in vitro. This finding is intriguing, as RTL2 was reported to impact the processing of a restricted subset of PolIV/RDR2 products (Elvira-Matelot et al. 2016), which are largely ~30- to 40-bp long (Blevins et al. 2015; Zhai et al. 2015). We suggest, therefore, that the criteria enabling RTL2-sensitivity of a subset of *Arabidopsis* RdDM targets (Elvira-Matelot et al. 2016) may be the production of PolIV/RDR2-dependent dsRNA precursors with sizes on the longer end of the distribution. Indeed, Figure 4 demonstrates that RTL2 enhances the accumulation of 24-nt siRNAs from 98-bp substrates, but not from 34-bp substrates, arguing that its cellular role could be to target longer PolIV/RDR2 products and make them more suitable substrates for DCL3. Further detailed characterization of RTL2 activities and affinities will be necessary to understand their biological roles. The BYL system represents a suitable approach toward this endeavor because various protein combinations can be tested together with RNA substrates of varying length, sequence, and/or structure, and the downstream output of DCL3 can be measured simultaneously. Furthermore, we show that the DRB7.1/DRB4 complex impairs RTL-mediated processing. This result highlights the general ability of DRBs to antagonize dsRNA cleavage by RNase III enzymes. In vitro results showed that the impairment of RTL1- and RTL2-mediated dsRNA cleavage did not lead to an increase in siRNA production, which is expected, as DCL activity was likewise impaired. It is conceivable, however, that DRB7.1/DRB4 could function in planta to sequester dsRNA away from RTL activities in a restricted time or location, and that this dsRNA could later be released and made available for dicing. In this way, dsRNA could be protected from RTL1-mediated silencing suppression, or also from viral RNases, which can act as silencing suppressors (Cuellar et al. 2009), and later be shunted into the DCL pathway.

In light of the broad and complex roles played by small RNAs in cellular regulation and the increasing intricacy of the multiple pathways governing their biogenesis, it will be important to further explore and define the biochemical and physiological contribution of RNA binding protein complexes to dsRNA processing.

MATERIALS AND METHODS

Plant material and growth conditions

Arabidopsis thaliana mutants *dcl4-2* and *drb4-1* in Col-0 ecotype and *drb7.1-1* (RIKEN 15-1848-1) in No-0 ecotype were described previously (Ito et al. 2002; Kuromori et al. 2004; Xie et al. 2005; Adenot et al. 2006; Nakazawa et al. 2007) and compared with their respective WT controls. Plants were grown on Klasmann substrate 2 soil in a controlled environment chamber (Kälte 3000) under the following conditions: 16 h light/8 h dark (140 µmol m^{-2} s^{-1} constant light intensity), constant temperature of 21°C, RH 60%.

Plasmid construction and plant transformation

DRB7.1 reporter plasmids were constructed by fusing the full-length genomic coding sequence of *DRB7.1* to its endogenous promoter, or the cDNA sequence of *DRB7.1* to the *Cauliflower mosaic virus* 35S promoter, and fusing a *2XFlag-2XHA* (*FHA*) or *GFP* encoding sequence at the 3′ position in pB7GW34 vector (Karimi et al. 2005) using the MultiSite Gateway Three-Fragment Vector Construction Kit (Invitrogen). Cloning primers are listed in Supplemental Table T1. Transgenic *Arabidopsis* were established by floral dip (Clough and Bent 1998). BiFC plasmids have been described previously (Clavel et al. 2016). Briefly, cDNA fragments of *DRB7.1*, *DRB4*, and *DCL2* were recombined into pBiFP1-4 vectors (Azimzadeh et al. 2008) using Gateway Technology (Invitrogen). For *DCL4*, the cDNA sequence was fused to the endogenous promoter and half *YFP* sequences in pB7GW34 (Karimi et al. 2005). DCL4-mCherry and RDR6-mCherry reporters were constructed by fusing an *mCherry* encoding sequence at the 3′ position to the full-length genomic coding sequence of *DCL4* or *RDR6* under the control of the *35S* promoter for *DCL4* or its endogenous promoter for *RDR6* in the pB7GW34 vector. Assembled vectors were introduced into *Agrobacterium tumefaciens* strain GV3101 and transient expression in *Nicotiana benthamiana* was performed as described previously (de Felippes and Weigel 2010). P38, an RNA silencing suppressor, was coexpressed to avoid silencing.

Immunoprecipitation

Fresh flower tissue from WT and transgenic *Arabidopsis* was ground in liquid nitrogen and homogenized in lysis buffer (50 mM Tris–HCl at pH 7.5, 150 mM NaCl, 10% glycerol, 0.1% v/v NP40) containing the EDTA-free protease inhibitor cocktail tablet (Roche) and MG132 in a buffer:tissue volume ratio of 3:1. Cell debris was removed by centrifugation for 15 min at 3000*g*, filtering through miracloth, and a subsequent centrifugation. The clarified lysate (input) was then incubated for 4 h with anti-Flag M2 red agarose beads (Sigma-Aldrich) and washed three times with 10 mL of lysis buffer. Proteins were eluted from agarose beads by competition with 3XFlag peptide (Sigma F4799) at 150 µg/mL in elution buffer (50 mM Tris–HCl at pH 7.5, 150 mM NaCl) and were subjected to Western blot and mass spectrometry analyses.

Mass spectrometry analysis

Immunoprecipitated samples were analyzed by the Functional Genomics Center of the University of Zürich (http://www.fgcz.ch/) using liquid chromatography electrospray ionization coupled with the tandem mass spectrometry (LC/ESI/MS/MS) detection method following proteolytic digestion. Database searches were carried out using the Mascot search program (Swiss-Prot, all species). Results were visualized and analyzed using Scaffold (Proteome Software). Parameters were set as follows, Protein Threshold: 99.0%, Min# Peptides: 1, Peptide Threshold: 50%.

Live-cell microscopy

Imaging was performed using a Zeiss 780 confocal laser scanning microscope with a 40× water immersion objective (LD C-Apochromat 40X/1.1). Fluorescence data from live, unsectioned tissues were acquired immediately after excision from the plant. Image data were analyzed and contrasted using Fiji software (Schindelin et al. 2012) and assembled with Adobe Photoshop CS6.

Protein analysis

Immunoprecipitation samples or proteins extracted from inflorescence tissue using TANAKA protocol (Hurkman and Tanaka 1986) were resolved by SDS–PAGE, then transferred onto an Immobilon-P PVDF membrane (Millipore). Membranes were blocked with 5% milk in PBS-Tween-20 0.1% (PBST) for 40 min and incubated overnight at 4°C with 1/5000 dilutions of primary antibodies rabbit anti-DCL4, guinea pig anti-DRB4, rat anti-GFP (Chromotek), and mouse anti-HA conjugated to horseradish peroxidase (Sigma). Membranes were washed four times with PBST, incubated 1 h at room temperature (except for anti-HA) in 5% milk with horseradish peroxidase-conjugated secondary antibodies and washed four times with PBST. Detection was performed using the ECL Plus Western Blotting Detection Reagents (GE Healthcare) and ChemiDoc Touch Imager (Bio-Rad). Image data were analyzed with Image Lab Software (Bio-Rad) and assembled in Adobe Photoshop CS6.

BYL in vitro translation

The tobacco BY-2 evacuolated protoplast lysate (BYL) was prepared as previously described (Komoda et al. 2004; Ishibashi et al. 2006) and the membrane fraction was preserved. *DRB7.1, DRB4, DRB2, RTL1*, and *RTL2* coding sequences were amplified by PCR and cloned into pSP64-poly(A) vector (Promega). *HA*/*Flag* epitopes were added during PCR using primers with overhangs encoding tag sequences. Primers are listed in Supplemental Table T1. Plasmids were linearized and mRNAs were in vitro transcribed using AmpliCap SP6 High Yield Message Maker Kit (Cellscript). In vitro translation was carried out as previously described (Ishibashi et al. 2006). Briefly, mRNAs (0.05 µg/µL or 120 nM) were mixed in BYL with 10× translation substrate buffer (7.5 mM ATP, 1 mM GTP, 250 mM creatine phosphate, 0.8 mM spermine, Amino Acid Mixture [Promega]), RiboLock RNase inhibitor (Thermo Scientific), creatine kinase 10mg/mL (Roche) and Translation Reaction (TR) buffer (30 mM HEPES-KOH, 80 mM KOAc, 1.8 mM $Mg(OAc)_2$, 2 mM DTT, pH 7.4). Mixtures were incubated 1–2 h at room temperature. One species of mRNA was translated per reaction.

Preparation of dsRNA

Radiolabeled dsRNA was prepared as described previously (Iki et al. 2017). Briefly, 34/36-nt dsRNA was prepared from two oligonucleotides (Gene Design). The 34-nt strand was end-labeled by incubation with [γ-^{32}P]-dATP and T4 PNK (Thermo Scientific), whereas 36-nt strand was end-phosphorylated without radiolabeling. Single-stranded RNAs were annealed as follows: Guide and passenger strand were mixed together with 5× annealing buffer (Tris–HCl [pH 7.6] 50 mM, KCl 100 mM, and $MgCl_2$ 5 mM) and incubated for 2 min at 96°C in a thermomixer (Eppendorf), at which point the machine was turned off and ssRNAs were left to anneal with decreasing temperature for 12 h. 98/100- and 510/512-nt dsRNA substrates were created by in vitro transcription of individual strands using the SP6-Scribe Standard RNA IVT kit (Cellscript) with [α-^{32}P]-CTP, purified on mini Quick Spin RNA Columns (Roche) and extracted with phenol:chloroform:isoamyl alcohol (PCI), followed by ethanol precipitation. Annealing of single-stranded RNA to obtain 98/100- and 510/512-nt dsRNA was achieved as described for 34/36-nt dsRNA species. All three species of duplexes contain a 5′ blunt end and 2 nt 3′ overhang.

dsRNA processing and binding assays

BYL containing in vitro-translated proteins were first mixed together in equimolar combinations as indicated, and subsequently incubated at room temperature with 10 nM of radiolabeled dsRNA with the addition of a 10× ATP-regenerating mix (75 mM ATP, 100 mM $MgCl_2$, 1 M creatine phosphate and 10 mg/mL creatine kinase). The reaction mixtures were diluted 0.5-fold in TE buffer (10 mM Tris, 1 mM EDTA, pH 8.0). RNA was extracted with equal volume of PCI and separated on native 15% polyacrylamide gels. Gels were dried using a Model 583 gel dryer (Bio-Rad). Signals were detected using the Typhoon FLA 9000 Image Analyzer (GE Healthcare). Band intensity quantification has been performed using Fiji software (https://fiji.sc/). Normalization is relative to the Mock controls (Supplemental Table T2).

For binding assays, BYL were mixed as indicated and one-third of the solution was removed as the protein input sample. Remaining BYL was incubated at room temperature for 7 min with radiolabeled dsRNA (3 nM of 34/36 nt, 15 nM of 98/100 nt, or 9 nM of 510/512 nt) with the addition of a 10× ATP-regenerating mix. A third of the volume was removed as the RNA input sample. Anti-Flag (Sigma) and anti-HA (ThermoScientific) magnetic beads were added to the remaining reaction mixture, incubated for 40 min at 4°C, washed 3× with TR buffer and resuspended in TE buffer. A fifth of the bead solution was taken as the immunoprecipitated protein sample. RNA was extracted from the remaining beads as the immunoprecipitated RNA sample.

RNA analysis

Arabidopsis inflorescences were frozen and ground. Total RNA was extracted using TRIzol (Invitrogen) and resuspended in 50% formamide solution. Analysis of low-molecular weight RNA was performed with 15–20 µg of total RNA separated on a 17.5% polyacrylamide–urea gel and electrotransferred to a HyBond-NX membrane (GE Healthcare). Membranes were chemically crosslinked with 1-ethyl-3-(3-dimethylaminopropyl) carbodiimide-mediated crosslinking (Pall and Hamilton 2008). DNA oligonucleotides complementary to U6, IR71, miRNAs, tasiRNAs or heterochromatic siRNAs were end-labeled by incubation with [γ-^{32}P]-dATP and T4 PNK (Thermo Scientific). IR2039 probe was radiolabeled by incubation of gel-purified PCR fragments with [α-^{32}P]-dCTP using the Prime-a-Gene labeling system (Promega). After each probe was detected with a Typhoon FLA 9000 (GE Healthcare), membranes were stripped twice with boiling 0.1% SDS buffer and rehybridized with a new probe. Probe sequences are listed in Supplemental Table T1. Band intensity quantification has been performed using Fiji software (https://fiji.sc/). Each band was first normalized to its corresponding U6 signal followed by normalization relative to the Wild-Type (Col-0) sample (Supplemental Table T2).

For Reverse Transcriptase quantitative PCR (qPCR), RNA was eluted in water following TRIzol extraction, treated with DNase I (Roche) and reverse-transcribed using the Maxima First-Strand cDNA synthesis kit (Thermo Scientific). qPCR was performed with a LightCycler 480 Instrument II (Roche) and the KAPA SYBR Fast qPCR Kit (KAPA Biosystems). Ct values were established by second derivative max calculated on three technical replicates per sample. Relative gene expression was calculated by ΔCt method using Actin2 or AT4G26410 as a control. Results were displayed as the average of indicated biological replicates with indicated error bars. qPCR primers are listed in Supplemental Table T1.

Bisulfite sequencing PCR (BSP)

Genomic DNA from wild-type seedlings as well as seedlings overexpressing DRB7.1 was extracted using the DNeasy Plant mini kit (QIAGEN) and treated with the EZ DNA Methylation-Gold Kit (Zymo Research) according to the manufacturer's instructions. Treated DNA was amplified using modified PCR conditions (Henderson et al. 2010) and gel purified with the GeneJET Gel Extraction Kit (Thermo Scientific). Primers were designed according to Henderson et al. (2010) and are listed in Supplemental Table T1. PCR fragments were ligated into pGEM-T easy vector and individual colonies were sequenced. DNA methylation analysis was performed through the online software Kismeth (Gruntman et al. 2008) (http://katahdin.mssm.edu/kismeth/revpage.pl). Of note, 95% confidence intervals were calculated using the Wilson score interval (Supplemental Table T3). Bisulfite-treated DNA fragments were analyzed from 21 individual colonies from WT and 23 from DRB7.1 overexpressor lines, each taken from two independent biological replicates and bulked for analysis.

SUPPLEMENTAL MATERIAL

Supplemental material is available for this article.

ACKNOWLEDGMENTS

The authors thank the following people for contributions: Peter Hunziker and the Functional Genomics Center Zürich for mass spectrometry analyses; Sylvain Bischof for advice on protein mass spectrometry; N.-H. Chua for DRB4-YFP-Flag plasmid; Yukuhide Fukuhara for the DRB4 antibody; Andre Imboden for assistance with plant growth; Gregory Schott and Andre

Imboden for maintaining BY-2 lysates; Florian Brioudes for providing pBiFP vectors; Olivier Voinnet and members of the group for insightful discussions and critical reading of the manuscript; and ETHZ ScopeM for microscopy facilities. This work was supported by the European Research Council (Frontiers of RNAi-II no. 323071 to Olivier Voinnet); the Eidgenössische Technische Hochschule Zürich (core grant to Olivier Voinnet); the European Molecular Biology Organization (ALTF 1487-2011 to N.P.); and a European Commission/Marie-Curie Actions Fellowship (IIF Project 299789 to N.P.).

Received October 12, 2016; accepted February 13, 2017.

REFERENCES

Adenot X, Elmayan T, Lauressergues D, Boutet S, Bouché N, Gasciolli V, Vaucheret H. 2006. DRB4-dependent TAS3 *trans*-acting siRNAs control leaf morphology through AGO7. *Curr Biol* **16:** 927–932.

Allen E, Xie Z, Gustafson AM, Sung GH, Spatafora JW, Carrington JC. 2004. Evolution of microRNA genes by inverted duplication of target gene sequences in *Arabidopsis thaliana*. *Nat Genet* **36:** 1282–1290.

Arribas-Hernández L, Marchais A, Poulsen C, Haase B, Hauptmann J, Benes V, Meister G, Brodersen P. 2016. The slicer activity of ARGONAUTE1 is required specifically for the phasing, not production, of *trans*-acting short interfering RNAs in *Arabidopsis*. *Plant Cell* **28:** 1563–1580.

Azimzadeh J, Nacry P, Christodoulidou A, Drevensek S, Camilleri C, Amiour N, Parcy F, Pastuglia M, Bouchez D. 2008. *Arabidopsis* TONNEAU1 proteins are essential for preprophase band formation and interact with centrin. *Plant Cell* **20:** 2146–2159.

Bernstein E, Caudy AA, Hammond SM, Hannon GJ. 2001. Role for a bidentate ribonuclease in the initiation step of RNA interference. *Nature* **409:** 363–366.

Blevins T, Rajeswaran R, Shivaprasad PV, Beknazariants D, Si-Ammour A, Park HS, Vazquez F, Robertson D, Meins F, Hohn T, et al. 2006. Four plant Dicers mediate viral small RNA biogenesis and DNA virus induced silencing. *Nucleic Acids Res* **34:** 6233–6246.

Blevins T, Podicheti R, Mishra V, Marasco M, Wang J, Rusch D, Tang H, Pikaard CS. 2015. Identification of Pol IV and RDR2-dependent precursors of 24 nt siRNAs guiding de novo DNA methylation in *Arabidopsis*. *Elife* **4:** e09591.

Bologna NG, Voinnet O. 2014. The diversity, biogenesis, and activities of endogenous silencing small RNAs in *Arabidopsis*. *Annu Rev Plant Biol* **65:** 473–503.

Borges F, Martienssen RA. 2015. The expanding world of small RNAs in plants. *Nat Rev Mol Cell Biol* **16:** 727–741.

Bouche N, Lauressergues D, Gasciolli V, Vaucheret H. 2006. An antagonistic function for *Arabidopsis* DCL2 in development and a new function for DCL4 in generating viral siRNAs. *EMBO J* **25:** 3347–3356.

Bracha-Drori K, Shichrur K, Katz A, Oliva M, Angelovici R, Yalovsky S, Ohad N. 2004. Detection of protein-protein interactions in plants using bimolecular fluorescence complementation. *Plant J* **40:** 419–427.

Clavel M, Pélissier T, Descombin J, Jean V, Picart C, Charbonel C, Saez-Vásquez J, Bousquet-Antonelli C, Deragon JM. 2015. Parallel action of AtDRB2 and RdDM in the control of transposable element expression. *BMC Plant Biol* **15:** 70.

Clavel M, Pélissier T, Montavon T, Tschopp MA, Pouch-Pélissier MN, Descombin J, Jean V, Dunoyer P, Bousquet-Antonelli C, Deragon JM. 2016. Evolutionary history of double-stranded RNA binding proteins in plants: identification of new cofactors involved in easiRNA biogenesis. *Plant Mol Biol* **91:** 131–147.

Clough SJ, Bent AF. 1998. Floral dip: a simplified method for Agrobacterium-mediated transformation of *Arabidopsis thaliana*. *Plant J* **16:** 735–743.

Comella P, Pontvianne F, Lahmy S, Vignols F, Barbezier N, Debures A, Jobet E, Brugidou E, Echeverria M, Sáez-Vásquez J. 2008. Characterization of a ribonuclease III-like protein required for cleavage of the pre-rRNA in the 3′ETS in *Arabidopsis*. *Nucleic Acids Res* **36:** 1163–1175.

Creasey KM, Zhai J, Borges F, Van Ex F, Regulski M, Meyers BC, Martienssen RA. 2014. miRNAs trigger widespread epigenetically activated siRNAs from transposons in *Arabidopsis*. *Nature* **508:** 411–415.

Cuellar WJ, Kreuze JF, Rajamaki ML, Cruzado KR, Untiveros M, Valkonen JP. 2009. Elimination of antiviral defense by viral RNase III. *Proc Natl Acad Sci* **106:** 10354–10358.

Curtin SJ, Watson JM, Smith NA, Eamens AL, Blanchard CL, Waterhouse PM. 2008. The roles of plant dsRNA-binding proteins in RNAi-like pathways. *FEBS Lett* **582:** 2753–2760.

de Felippes FF, Weigel D. 2010. Transient assays for the analysis of miRNA processing and function. *Methods Mol Biol* **592:** 255–264.

Deleris A, Gallego-Bartolome J, Bao J, Kasschau KD, Carrington JC, Voinnet O. 2006. Hierarchical action and inhibition of plant Dicer-like proteins in antiviral defense. *Science* **313:** 68–71.

Diaz-Pendon JA, Li F, Li WX, Ding SW. 2007. Suppression of antiviral silencing by cucumber mosaic virus 2b protein in *Arabidopsis* is associated with drastically reduced accumulation of three classes of viral small interfering RNAs. *Plant Cell* **19:** 2053–2063.

Dong Z, Han MH, Fedoroff N. 2008. The RNA-binding proteins HYL1 and SE promote accurate in vitro processing of pri-miRNA by DCL1. *Proc Natl Acad Sci* **105:** 9970–9975.

Dunoyer P, Himber C, Voinnet O. 2005. DICER-LIKE 4 is required for RNA interference and produces the 21-nucleotide small interfering RNA component of the plant cell-to-cell silencing signal. *Nat Genet* **37:** 1356–1360.

Eamens AL, Smith NA, Curtin SJ, Wang MB, Waterhouse PM. 2009. The *Arabidopsis thaliana* double-stranded RNA binding protein DRB1 directs guide strand selection from microRNA duplexes. *RNA* **15:** 2219–2235.

Eamens AL, Kim KW, Curtin SJ, Waterhouse PM. 2012a. DRB2 is required for microRNA biogenesis in *Arabidopsis thaliana*. *PLoS One* **7:** e35933.

Eamens AL, Wook Kim K, Waterhouse PM. 2012b. DRB2, DRB3 and DRB5 function in a non-canonical microRNA pathway in *Arabidopsis thaliana*. *Plant Signal Behav* **7:** 1224–1229.

Elvira-Matelot E, Hachet M, Shamandi N, Comella P, Sáez-Vásquez J, Zytnicki M, Vaucheret H. 2016. *Arabidopsis* RNASE THREE LIKE2 modulates the expression of protein-coding genes via 24-nucleotide small interfering RNA-directed DNA methylation. *Plant Cell* **28:** 406–425.

Endo Y, Iwakawa HO, Tomari Y. 2013. *Arabidopsis* ARGONAUTE7 selects miR390 through multiple checkpoints during RISC assembly. *EMBO Rep* **14:** 652–658.

Fahlgren N, Howell MD, Kasschau KD, Chapman EJ, Sullivan CM, Cumbie JS, Givan SA, Law TF, Grant SR, Dangl JL, et al. 2007. High-throughput sequencing of *Arabidopsis* microRNAs: evidence for frequent birth and death of MIRNA genes. *PLoS One* **2:** e219.

Fukudome A, Kanaya A, Egami M, Nakazawa Y, Hiraguri A, Moriyama H, Fukuhara T. 2011. Specific requirement of DRB4, a dsRNA-binding protein, for the in vitro dsRNA-cleaving activity of *Arabidopsis* Dicer-like 4. *RNA* **17:** 750–760.

Fusaro AF, Matthew L, Smith NA, Curtin SJ, Dedic-Hagan J, Ellacott GA, Watson JM, Wang MB, Brosnan C, Carroll BJ, et al. 2006. RNA interference-inducing hairpin RNAs in plants act through the viral defence pathway. *EMBO Rep* **7:** 1168–1175.

Gasciolli V, Mallory AC, Bartel DP, Vaucheret H. 2005. Partially redundant functions of *Arabidopsis* DICER-like enzymes and a role for DCL4 in producing *trans*-acting siRNAs. *Curr Biol* **15:** 1494–1500.

Gruntman E, Qi Y, Slotkin RK, Roeder T, Martienssen RA, Sachidanandam R. 2008. Kismeth: analyzer of plant methylation states through bisulfite sequencing. *BMC Bioinformatics* **9:** 371.

Ha M, Kim VN. 2014. Regulation of microRNA biogenesis. *Nat Rev Mol Cell Biol* **15:** 509–524.

Henderson IR, Zhang X, Lu C, Johnson L, Meyers BC, Green PJ, Jacobsen SE. 2006. Dissecting *Arabidopsis thaliana* DICER function in small RNA processing, gene silencing and DNA methylation patterning. *Nat Genet* **38:** 721–725.

Henderson IR, Chan SR, Cao X, Johnson L, Jacobsen SE. 2010. Accurate sodium bisulfite sequencing in plants. *Epigenetics* **5:** 47–49.

Hiraguri A, Itoh R, Kondo N, Nomura Y, Aizawa D, Murai Y, Koiwa H, Seki M, Shinozaki K, Fukuhara T. 2005. Specific interactions between Dicer-like proteins and HYL1/DRB-family dsRNA-binding proteins in *Arabidopsis thaliana*. *Plant Mol Biol* **57:** 173–188.

Hurkman WJ, Tanaka CK. 1986. Solubilization of plant membrane proteins for analysis by two-dimensional gel electrophoresis. *Plant Physiol* **81:** 802–806.

Iki T, Yoshikawa M, Nishikiori M, Jaudal MC, Matsumoto-Yokoyama E, Mitsuhara I, Meshi T, Ishikawa M. 2010. In vitro assembly of plant RNA-induced silencing complexes facilitated by molecular chaperone HSP90. *Mol Cell* **39:** 282–291.

Iki T, Yoshikawa M, Meshi T, Ishikawa M. 2012. Cyclophilin 40 facilitates HSP90-mediated RISC assembly in plants. *EMBO J* **31:** 267–278.

Iki T, Tschopp MA, Voinnet O. 2017. Biochemical and genetic functional dissection of the P38 viral suppressor of RNA silencing. *RNA* (this issue) **23:** 639–654.

Ishibashi K, Komoda K, Ishikawa M. 2006. In vitro translation and replication of tobamovirus RNA in a cell-free extract of evacuolated tobacco BY-2 protoplasts. In *Biotechnology in agriculture and forestry* (ed. Nagata T, et al.), pp. 183–194. Springer, Berlin.

Ito T, Motohashi R, Kuromori T, Mizukado S, Sakurai T, Kanahara H, Seki M, Shinozaki K. 2002. A new resource of locally transposed dissociation elements for screening gene-knockout lines in silico on the *Arabidopsis* genome. *Plant Physiol* **129:** 1695–1699.

Iwakawa HO, Tomari Y. 2013. Molecular insights into microRNA-mediated translational repression in plants. *Mol Cell* **52:** 591–601.

Jakubiec A, Yang SW, Chua NH. 2012. *Arabidopsis* DRB4 protein in antiviral defense against Turnip yellow mosaic virus infection. *Plant J* **69:** 14–25.

Jouannet V, Moreno AB, Elmayan T, Vaucheret H, Crespi MD, Maizel A. 2012. Cytoplasmic *Arabidopsis* AGO7 accumulates in membrane-associated siRNA bodies and is required for ta-siRNA biogenesis. *EMBO J* **31:** 1704–1713.

Karimi M, De Meyer B, Hilson P. 2005. Modular cloning in plant cells. *Trends Plant Sci* **10:** 103–105.

Komoda K, Naito S, Ishikawa M. 2004. Replication of plant RNA virus genomes in a cell-free extract of evacuolated plant protoplasts. *Proc Natl Acad Sci* **101:** 1863–1867.

Kumakura N, Takeda A, Fujioka Y, Motose H, Takano R, Watanabe Y. 2009. SGS3 and RDR6 interact and colocalize in cytoplasmic SGS3/RDR6-bodies. *FEBS Lett* **583:** 1261–1266.

Kurihara Y, Watanabe Y. 2004. *Arabidopsis* micro-RNA biogenesis through Dicer-like 1 protein functions. *Proc Natl Acad Sci* **101:** 12753–12758.

Kurihara Y, Takashi Y, Watanabe Y. 2006. The interaction between DCL1 and HYL1 is important for efficient and precise processing of pri-miRNA in plant microRNA biogenesis. *RNA* **12:** 206–212.

Kuromori T, Hirayama T, Kiyosue Y, Takabe H, Mizukado S, Sakurai T, Akiyama K, Kamiya A, Ito T, Shinozaki K. 2004. A collection of 11 800 single-copy *Ds* transposon insertion lines in *Arabidopsis*. *Plant J* **37:** 897–905.

Lakatos L, Csorba T, Pantaleo V, Chapman EJ, Carrington JC, Liu YP, Dolja VV, Calvino LF, López-Moya JJ, Burgyán J. 2006. Small RNA binding is a common strategy to suppress RNA silencing by several viral suppressors. *EMBO J* **25:** 2768–2780.

Law JA, Jacobsen SE. 2010. Establishing, maintaining and modifying DNA methylation patterns in plants and animals. *Nat Rev Genet* **11:** 204–220.

Lee HY, Zhou K, Smith AM, Noland CL, Doudna JA. 2013. Differential roles of human Dicer-binding proteins TRBP and PACT in small RNA processing. *Nucleic Acids Res* **41:** 6568–6576.

Martínez de Alba AE, Elvira-Matelot E, Vaucheret H. 2013. Gene silencing in plants: a diversity of pathways. *Biochim Biophys Acta* **1829:** 1300–1308.

Matzke MA, Kanno T, Matzke AJ. 2014. RNA-directed DNA methylation: the evolution of a complex epigenetic pathway in flowering plants. *Annu Rev Plant Biol* **66:** 243–267.

Moissiard G, Parizotto EA, Himber C, Voinnet O. 2007. Transitivity in *Arabidopsis* can be primed, requires the redundant action of the antiviral Dicer-like 4 and Dicer-like 2, and is compromised by viral-encoded suppressor proteins. *RNA* **13:** 1268–1278.

Montavon T, Kwon Y, Zimmermann A, Hammann P, Vincent T, Cognat V, Michel F, Dunoyer P. 2016. A specific dsRNA-binding protein complex selectively sequesters endogenous inverted-repeat siRNA precursors and inhibits their processing. *Nucleic Acids Res* **45:** 1330–1344.

Mosher RA, Melnyk CW, Kelly KA, Dunn RM, Studholme DJ, Baulcombe DC. 2009. Uniparental expression of PolIV-dependent siRNAs in developing endosperm of *Arabidopsis*. *Nature* **460:** 283–286.

Nagano H, Fukudome A, Hiraguri A, Moriyama H, Fukuhara T. 2014. Distinct substrate specificities of *Arabidopsis* DCL3 and DCL4. *Nucleic Acids Res* **42:** 1845–1856.

Nakazawa Y, Hiraguri A, Moriyama H, Fukuhara T. 2007. The dsRNA-binding protein DRB4 interacts with the Dicer-like protein DCL4 in vivo and functions in the trans-acting siRNA pathway. *Plant Mol Biol* **63:** 777–785.

Pall GS, Hamilton AJ. 2008. Improved northern blot method for enhanced detection of small RNA. *Nat Protoc* **3:** 1077–1084.

Parent JS, Bouteiller N, Elmayan T, Vaucheret H. 2015. Respective contributions of *Arabidopsis* DCL2 and DCL4 to RNA silencing. *Plant J* **81:** 223–232.

Park W, Li J, Song R, Messing J, Chen X. 2002. CARPEL FACTORY, a Dicer homolog, and HEN1, a novel protein, act in microRNA metabolism in *Arabidopsis thaliana*. *Curr Biol* **12:** 1484–1495.

Pelissier T, Clavel M, Chaparro C, Pouch-Pelissier MN, Vaucheret H, Deragon JM. 2011. Double-stranded RNA binding proteins DRB2 and DRB4 have an antagonistic impact on polymerase IV-dependent siRNA levels in *Arabidopsis*. *RNA* **17:** 1502–1510.

Pumplin N, Sarazin A, Jullien PE, Bologna NG, Oberlin S, Voinnet O. 2016. DNA methylation influences the expression of DICER-LIKE4 isoforms, which encode proteins of alternative localization and function. *Plant Cell* **28:** 2786–2804.

Qi Y, Denli AM, Hannon GJ. 2005. Biochemical specialization within *Arabidopsis* RNA silencing pathways. *Mol Cell* **19:** 421–428.

Qu F, Ye X, Morris TJ. 2008. *Arabidopsis* DRB4, AGO1, AGO7, and RDR6 participate in a DCL4-initiated antiviral RNA silencing pathway negatively regulated by DCL1. *Proc Natl Acad Sci* **105:** 14732–14737.

Raja P, Jackel JN, Li S, Heard IM, Bisaro DM. 2014. *Arabidopsis* double-stranded RNA binding protein DRB3 participates in methylation-mediated defense against geminiviruses. *J Virol* **88:** 2611–2622.

Rajagopalan R, Vaucheret H, Trejo J, Bartel DP. 2006. A diverse and evolutionarily fluid set of microRNAs in *Arabidopsis thaliana*. *Genes Dev* **20:** 3407–3425.

Reinhart BJ, Weinstein EG, Rhoades MW, Bartel B, Bartel DP. 2002. MicroRNAs in plants. *Genes Dev* **16:** 1616–1626.

Reis RS, Hart-Smith G, Eamens AL, Wilkins MR, Waterhouse P. 2015. Gene regulation by translational inhibition is determined by Dicer partnering proteins. *Nat Plants* **1:** 14027.

Schauer SE, Jacobsen SE, Meinke DW, Ray A. 2002. DICER-LIKE1: blind men and elephants in *Arabidopsis* development. *Trends Plant Sci* **7:** 487–491.

Schindelin J, Arganda-Carreras I, Frise E, Kaynig V, Longair M, Pietzsch T, Preibisch S, Rueden C, Saalfeld S, Schmid B, et al. 2012. Fiji: an open-source platform for biological-image analysis. *Nat Methods* **9:** 676–682.

Shamandi N, Zytnicki M, Charbonnel C, Elvira-Matelot E, Bochnakian A, Comella P, Mallory AC, Lepère G, Sáez-Vásquez J,

Vaucheret H. 2015. Plants encode a general siRNA suppressor that is induced and suppressed by viruses. *PLoS Biol* **13:** e1002326.

Vazquez F, Vaucheret H, Rajagopalan R, Lepers C, Gasciolli V, Mallory AC, Hilbert JL, Bartel DP, Crété P. 2004. Endogenous *trans*-acting siRNAs regulate the accumulation of *Arabidopsis* mRNAs. *Mol Cell* **16:** 69–79.

Xie Z, Johansen LK, Gustafson AM, Kasschau KD, Lellis AD, Zilberman D, Jacobsen SE, Carrington JC. 2004. Genetic and functional diversification of small RNA pathways in plants. *PLoS Biol* **2:** E104.

Xie Z, Allen E, Wilken A, Carrington JC. 2005. DICER-LIKE 4 functions in *trans*-acting small interfering RNA biogenesis and vegetative phase change in *Arabidopsis thaliana*. *Proc Natl Acad Sci* **102:** 12984–12989.

Ye R, Wang W, Iki T, Liu C, Wu Y, Ishikawa M, Zhou X, Qi Y. 2012. Cytoplasmic assembly and selective nuclear import of *Arabidopsis* Argonaute4/siRNA complexes. *Mol Cell* **46:** 859–870.

Yoshikawa M, Peragine A, Park MY, Poethig RS. 2005. A pathway for the biogenesis of *trans*-acting siRNAs in *Arabidopsis*. *Genes Dev* **19:** 2164–2175.

Yoshikawa M, Iki T, Tsutsui Y, Miyashita K, Poethig RS, Habu Y, Ishikawa M. 2013. 3′ fragment of miR173-programmed RISC-cleaved RNA is protected from degradation in a complex with RISC and SGS3. *Proc Natl Acad Sci* **110:** 4117–4122.

Zhai J, Bischof S, Wang H, Feng S, Lee TF, Teng C, Chen X, Park SY, Liu L, Gallego-Bartolome J, et al. 2015. A one precursor one siRNA model for Pol IV-dependent siRNA biogenesis. *Cell* **163:** 445–455.

A complex of *Arabidopsis* DRB proteins can impair dsRNA processing

Marie-Aude Tschopp, Taichiro Iki, Christopher A. Brosnan, et al.

RNA 2017 23: 782-797 originally published online February 23, 2017
Access the most recent version at doi:10.1261/rna.059519.116